

Estimated spectrum of a 6MV X-ray

Myung Jin Yoo, Ph. D.

Kosin Medical College and Medical Center, Pusan, Korea

Abstract

The quality of radiation for a high energy x-ray beam can be specified by its attenuation curve in a selected material. The inverse Laplace transform of the attenuation curve can be used as an approximate indication of the energy spectrum of the beam. We have made a comparative investigation of the estimated spectrum obtained by the Laplace transform analysis of the transmitted exposure data measured in an absorption study of a 6MV x-ray beam. Two of existing transform pair models have been investigated and discussed.

INTRODUCTION

Rapid advances in diagnostic radiology,^{1,2)} therapeutic radiology^{3,4)} and other areas of physics⁵⁾ have sparked renewed interest in methods of determining x-ray spectrum.

Ordinarily, the necessary spectral information is obtained by one of two methods. The standard method involves direct measurements using a (single or multi channel) pulse height analyzer.⁶⁾ Unfortunately, this approach requires expensive, highly specialized equipment. Also it is hardly suited for the confined space and time available in the clinic.

The alternative method involves inferring spectral information from attenuation measurements⁷⁾. The most common approach is to describe the beam in terms of an "effective energy" based upon the half value layer(HVL) in some appropriate substance. Physically, this corresponds to approximating the spectrum by a single spike at that energy which happens to yield the observed HVL. The second HVL can be used to improve this approximation ; but the result may or may not resemble the actual spectrum.

In principle, an examination of the entire attenuation curves should enable one to completely reconstruct the corresponding spectrum.

Although high energy medical accelerators have been widely used in radiation therapy for many years, only a few measurements of bremsstrahlung spectrum above 2MV have been reported.^{3,4,8,9)}

The purpose of the present paper is to evaluate the usefulness of the Laplace transform method as representation of the spectrum for a 6MV x-ray.

MATERIALS AND METHOD

1. Experiment

Figure 1 shows the experimental setup for the attenuation measurements of the 6MV x-rays from a linear accelerator with a Capintec PR-06C (volume 0.65ml) ionization chamber.

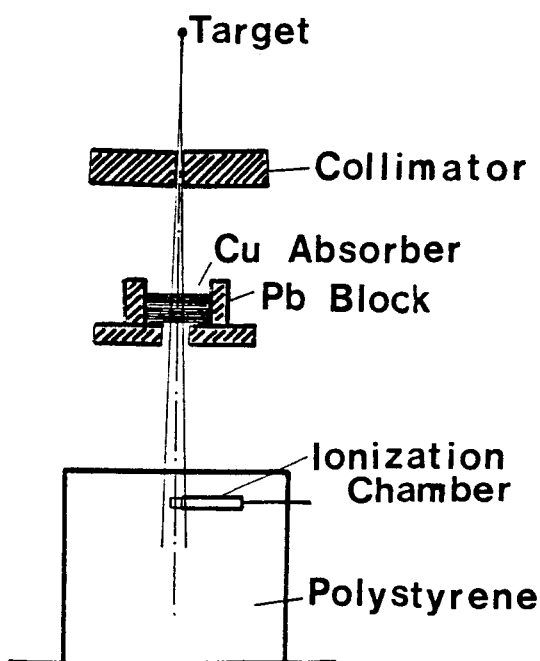


Figure 1. Experimental setup for attenuation measurements.

Scattered radiation from the collimators and other structures near the x-ray target in the accelerator was reduced by a thick lead block.

The field size, determined by the collimators in the accelerator, was $3 \times 3 \text{ cm}^2$ at the chamber, placed at 100cm distance from the focus. This field size was just large enough to include the chamber in the region of the beam unaffected by penumbra.

The absorbers used in the experiment were copper sheets 5.824 gcm^{-2} thick.

A purity of 99.9% was certified by the supplier. The absorber thickness was varied in 25 steps up to 145.6 gcm^{-2} . The copper sheets were sequentially placed over a thin Lucite tray with a 5-cm-diam hole in the center.

The results are shown in Figure 2 as triangle.

2. Theory

The relative transmitted exposure is

$$T(x) = \frac{I(x)}{I(0)} = \int_0^E F(E) e^{-\mu(E)x} dE, \quad (1)$$

where $F(E)$ is the fractional signal due to the photons of energy E , x is the thickness (gcm^{-2}) of the absorber, and $\mu(E)$ is the mass attenuation coefficient (cm^2g^{-1}) of the absorber material.

We can change the variable of integration from E to $\mu(E)$ by introducing another fractional signal function, called by Baird the prespectrum,

$$P(\mu) = -F(E) \frac{dE}{d\mu} \quad (2)$$

Thus the relative transmitted exposure is given by

$$T(x) = \int_0^\infty P(\mu) e^{-\mu x} d\mu, \quad (3)$$

where the limits of integration are the extrapolated values of μ : $\mu(0) = \infty$, and $\mu(\infty) = 0$.

The functions $T(x)$ and $P(\mu)$ form a Laplace transform pair, and if either is known, the other can be determined.

The energy fluence $S(E)$ is given by

$$S(E) = \frac{I(0)F(E)}{R(E)\mu_{en}(E)}, \quad (4)$$

where $R(E)$ is energy response function, and $\mu_{en}(E)$ is the mass energy absorption coefficient (cm^2g^{-1}).

3. Laplace transform pair models

Jones model

$$T(x) \simeq T_1(x) = \exp[-\mu_m x - B(\sqrt{x+d} - \sqrt{d})]. \quad (5)$$

$$P(\mu) = (B/2\sqrt{\pi})(\mu - \mu_m)^{-2/3} \exp[B\sqrt{d} - (\mu - \mu_m)d - B^2/4(\mu - \mu_m)]. \quad (6)$$

Jones introduced,

$$y = -\ln[T(x)e^{\mu_m x}]. \quad (7)$$

If $T_1(x)$ of Eq. (5) truly represents the measured attenuation data $T(x)$, it follows that

$$\frac{x}{y} = B^{-2}y + \frac{2\sqrt{d}}{B} \quad (8)$$

This model for $T(x)$ produces a straight line of x/y vs y with slope B^{-2} and the intercept with the x/y axis $2\sqrt{d}/B$.

Huang-Kase-Bjargard model

$$T(x) \simeq T_2(x) = \exp(-ax + bx^2) \quad (9)$$

$$P(\mu) = \frac{1}{2\sqrt{\pi b}} \exp[-(\mu - a)^2/4b]. \quad (10)$$

one can easily show that

$$\mu(x) = \frac{1}{T} \left(- \frac{dT}{dx} \right) \quad (11)$$

by Eq. (3).

Using Eq.(9) and (11), we get that $\mu(0)=a$.

This model for $T(x)$ produces a straight line of $\mu(x)$ vs x with slope $-2b$ and the intercept with the $\mu(x)$ axis a .

4. Energy response function

Johns and Cunningham¹⁰⁾ have discussed the response function of an ion chamber. Since we used an air equivalent plastic(a. e. p.) wall ion chamber, with a polystyrene buildup cap, we have employed a modification of their Eq. (7.32) to get

$$R(E) = \frac{(\bar{\mu}_{ab})_{air}^{a.e.p.} K(c\rho_{a.e.p.}) K(d\rho_{polystyrene})}{(\bar{S})_{air}^{a.e.p.} K(a\rho_{a.e.p.}) K(c\rho_{polystyrene})}, \quad (12)$$

where a constant of proportionality has been omitted, and all quantities are energy dependent variables. In Eq.(12), $(\bar{\mu}_{ab})_{air}^{a.e.p.}$ is the average mass absorption coefficient ratio, and $(\bar{S})_{air}^{a.e.p.}$, the average mass stopping power ratio, for a.e.p. to air. Each factor $K(r\rho_{med})$ is an effective attenuation factor for a cylinder of a material "med" and a radius r . ρ_{med} is the density of the wall or cap material ; a , c , and d are the radii of the air cavity, ion chamber thimble, and buildup cap, respectively. The values of all quantities appearing in Eq.(12) are obtainable from the Tables A5 and A7, and Figure 7.5 in Johns and Cunningham. The parameter values for our ion chamber and buildup cap are ; $\rho_{polystyrene} = 1.044 \text{gcm}^{-3}$, $\rho_{a.e.p.} = 1.8 \times 10^{-3} \text{gcm}^{-3}$, $a = 0.08$ cm, $c = 0.35$ cm and $d = 0.85$ cm.

5. $d\mu/dE$, and μ_{en}

We have used the tables of photon interactions by Hubbel¹¹⁾ for the values of for copper, and μ_{en} for air. The values of $d\mu/dE$ for copper, over the entire range of energy, were calculated from the same μ -E tables.

RESULTS

Figure 2 shows that two models provide simulation of the measured transmission data.

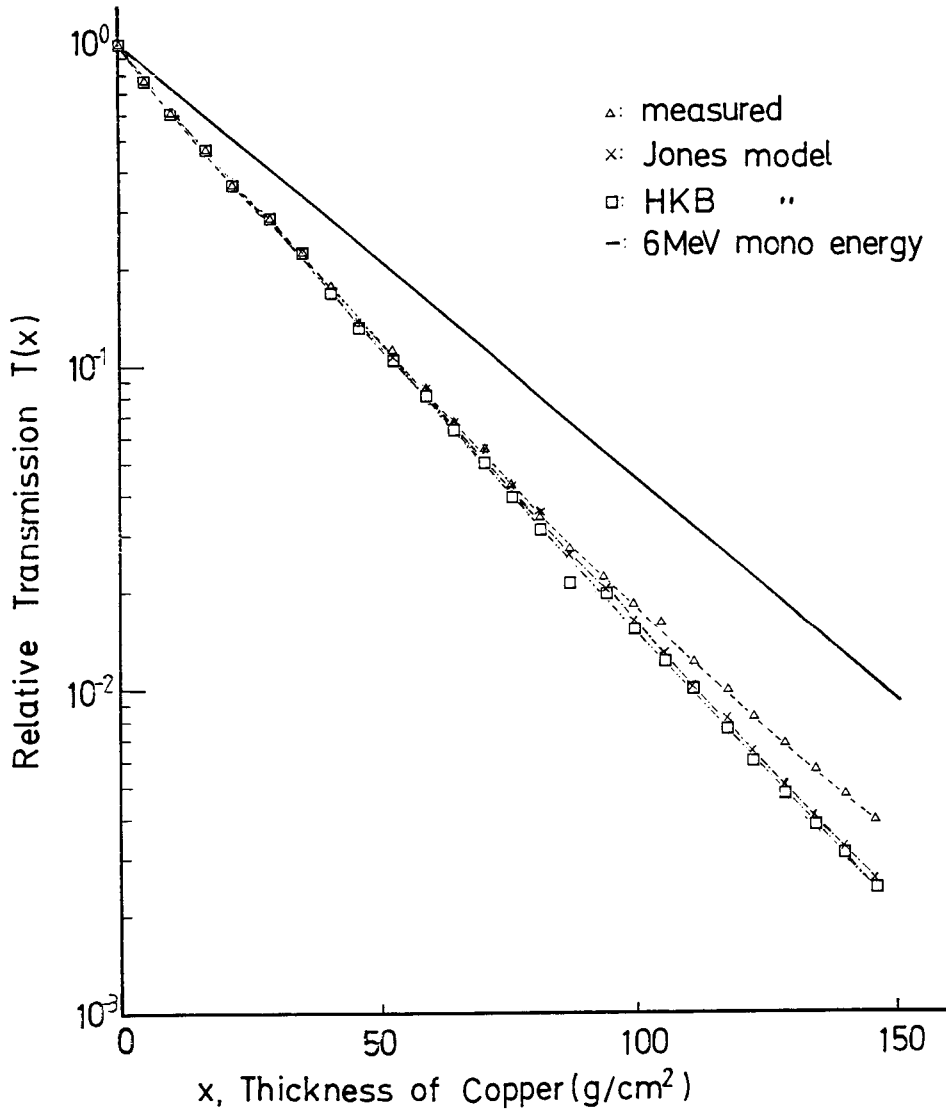


Fig. 2. Relative transmission $T(x)$ vs thickness of copper x .

To apply Jones method of analysis to the measured 6MV data, it is required to choose a value for μ_m for use in Eq.(5) through(8). Assuming that the maximum photon energy is 6MeV, $\mu_m = 0.0318 \text{cm}^2 \text{g}^{-1}$.

In Figure 3, the plot intercepts the x/y axis at 78.5gcm^{-2} and is linear between 100% and about 10% transmission. But the plot deviates from a straight line as relative transmission falls below 10%. When examining the use of Jones's technique critically, one can conclude from Fig. 3 that Eq.(5) will be a poor fit to the transmission data for $T < 0.1$ the two parameters needed for the fit expressed by Eq.(5) can be extracted from Fig. 3 as $B = 0.25 \text{cmg}^{-1/2}$ and

$d = 94.33 \text{ gcm}^{-2}$.

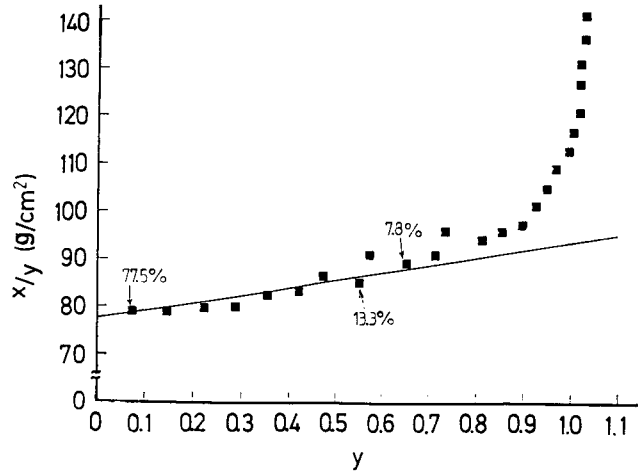


Fig. 3. Plot of x/y vs y for the measured transmission data.

Using these values, the $P(\mu)$ distribution [Eq.(6)] is defined as well as the $F(E)$ spectrum [Eq.(2)].

Figure 4 shows $\bar{\mu}(x)$, defined as $(1/T)(-dT/dx)$, as a function of the attenuator thickness x .

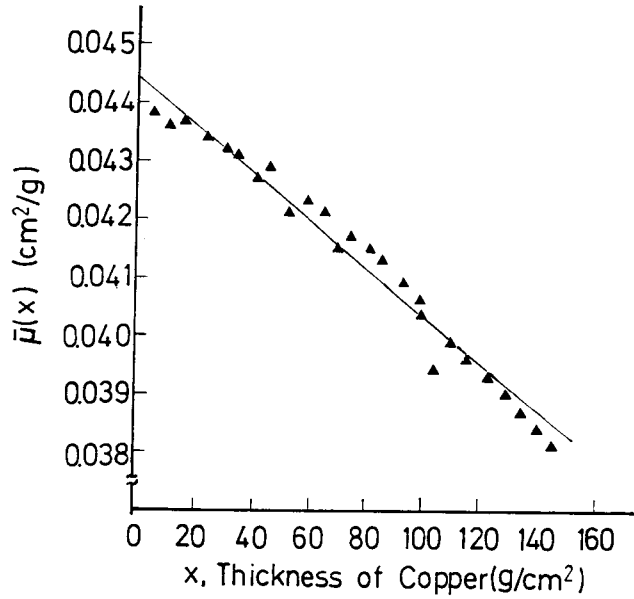


Fig. 4. $\bar{\mu}(x)$ in copper vs thickness of copper x .

To apply HKB method of analysis to the measured 6MV data, it is required to choose the values for a and b for use in Eq.(9) and (10). The two parameters needed for the fit expressed by Eq.(9) can be extracted from Fig. 4 as $a=0.04443\text{cm}^2\text{g}^{-1}$ and $b=2.08\times 10^{-5}\text{cm}^4\text{g}^{-2}$.

Figure 5 shows $P(\mu)$ as a function of μ reconstructed from the measured attenuation data using Eq.(6) and Eq.(10).

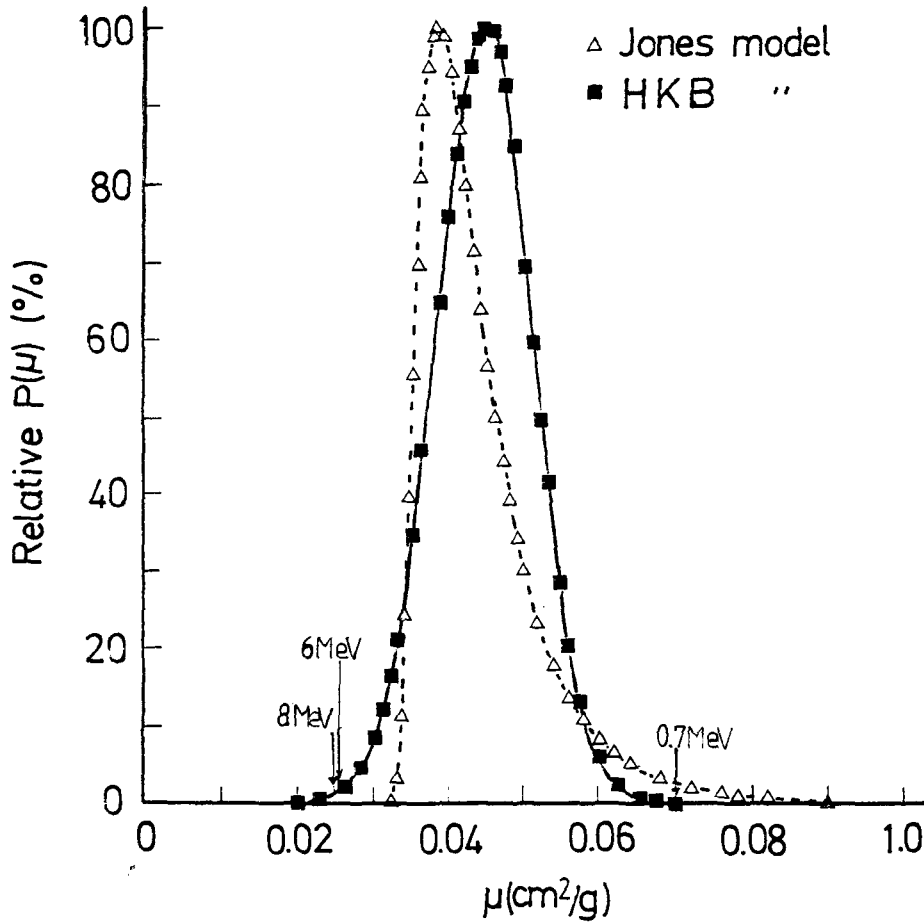


Fig. 5. Relative $P(\mu)$ as a function of attenuation coefficient μ in copper.

In this figure, the solid curve and the dashed curve given the prespectrum form the HKB model and the Jones model, respectively.

In case of HKB model, the mean attenuation coefficient of $0.04443\text{cm}^2\text{g}^{-1}$ corresponds to a photon energy of 1.7MeV.

Energy fluence spectrum $S(E)$ was calculated from $P(\mu)$, Eq.(2), and Eq.(4).

It is included in figure 6.

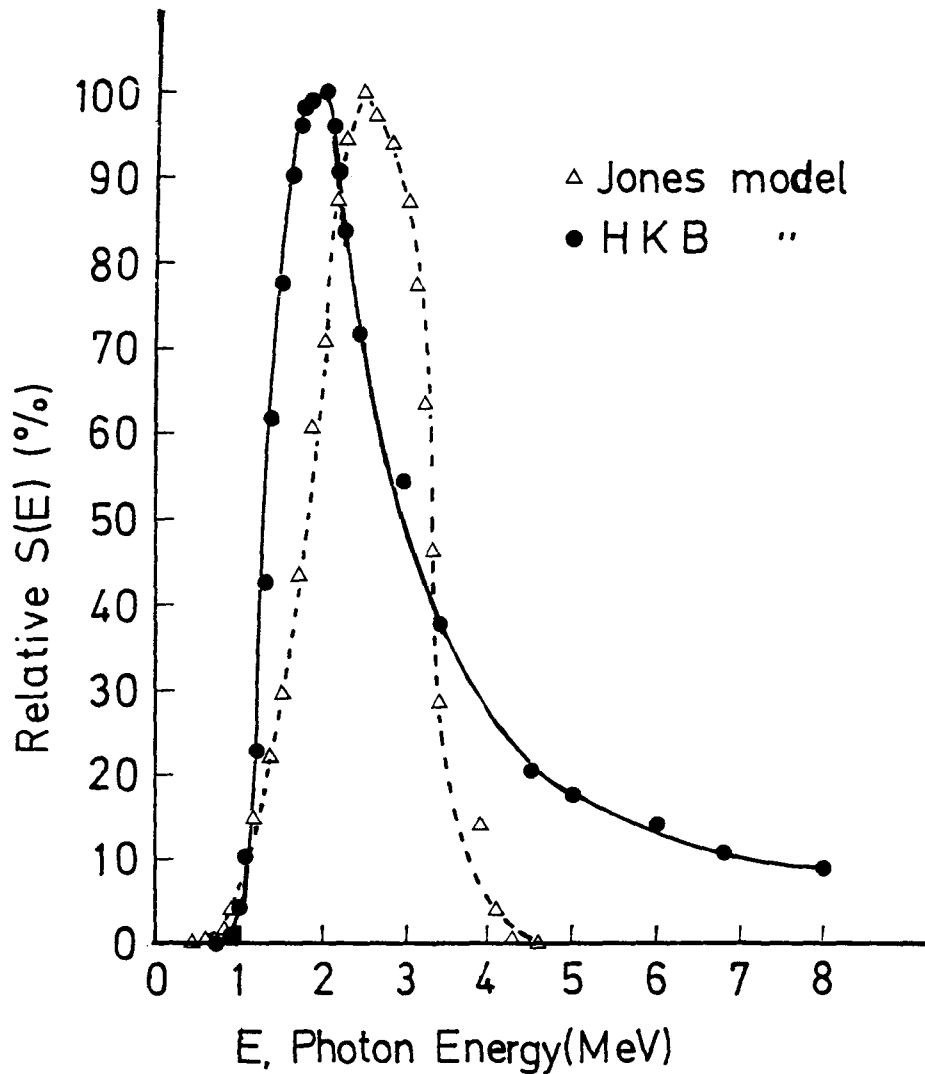


Fig. 6. Relative energy fluence $S(E)$ as a function of photon energy E .

In this figure, the solid curve gives the energy fluence $S(E)$ as a function of photon energy E reconstructed from the HKB model, represented by Eq.(9) and Eq.(10). The low energy cutoff is 1.99MeV, and a small tail extends beyond 6MeV. The figure also gives the spectrum determined from Jones model and shows the low energy cutoff at 0.45MeV the most probable energy is 2.45MeV and no detectable energy higher than about 4.6MeV

DISCUSSION

As shown by Figure 3 Jones's Eq.(5) gives a poor fit to the measured transmission data for $T < 0.1$ with deviations that increase as the transmission decreases. When reexamining the basic assumptions made by Jones, the deviations for low transmission values are not surprising. It can be shown theoretically that as the slope of $\ln T(s)$ approaches $-\mu m$ for small transmission values, y will approach a constant value and x/y will steadily increase, i. e., the behavior suggested by Fig. 3. In the result, as seen in Fig. 6, $S(E)$ shows no detectable energy higher than about 4.6MeV.

In the HKB model, the fit of the transmission data to a second order polynomial is highly satisfactory. However, the utility of the second order polynomial fit for the transmission, and the normal distribution for the spectrum $p(\mu)$ is likely to be a somewhat different consequence of the shape of the true energy spectrum.

This surfaces in Fig. 5, which shows that the technique assigns 2.5% of the chamber response to photons with attenuation coefficient values lower than that for 8MeV. This clearly is impossible, because μ has the minimum value at 8MeV for copper and lower values simply do not occur¹¹⁾. Also, no photons should have energy appreciably higher than 6MeV, since the x-ray machine measured is a 6MV linear accelerator, but the reconstruction assigns 3% of the chamber response to such photons. these inconsistencies are the result of the choice of the fit Eq.(9), which means that $P(\mu)$ will be represented by a Gaussian function, which has long tails for small and large μ values³⁾

In Addition, the measurement accuracy must be considered. The possible errors in the measurement of transmission are believed to be small, and were estimated to be $\pm 2.5\%$ at 0.01 $T(x)$ and $\pm 6\%$ at 0.02 $T(x)$.

The energy dependence of the detector is estimated to be known within a few percent.

These errors affect the results only in the final stage, represented by the transition from differential chamber response $F(E)$ in Eq. (2) to the energy fluence spectrum $S(E)$ in Fig. 6. In fact, by the reasons mentioned above, the reconstruction of HKB model assigns 12% of $S(E)$ at energy higher than 6MeV.

CONCLUSION

The spectral distribution reconstructed by a Laplace transformation of transmission data is forced by the fundamental mathematical assumptions to take on a shape that may or may not be a good representation of the true spectrum.

Jones's method of attenuation analysis to characterize the beam quality and represent the approximate spectral shape for 6MV x-rays has been shown to have severe limitations.

HKB technique, using a second order polynomial to model the measured transmission data, was able to reflect the experimental results with high fidelity. But the attenuation analysis

does not result in a perfect representation of the true spectrum, we need notice especially the shape of $p(\mu)$ and the tail above 6MeV.

In the near future, we have plans to study any other Laplace transform pair models except two models used in this paper to obtain the estimated spectrum for 6MV x-ray. Also, to evaluate the estimated spectrum for 6MV x-ray, we have plans to compare Laplace transform method with Monte Carlo method.

REFERENCES

1. Archer BR, Wagner LK : Determination of diagnostic x-ray spectra with characteristic radiation using attenuation analysis. *Med Phys* 15 : 637–641, 1988.
2. Hunag PH, Chen TS, Kase KR : Reconstruction of diagnostic x-ray spectra by numerical analysis of transmission data. *Med Phys* 13 : 707–710, 1986.
3. Huang PH, Kase KR, Bjangard BE : Reconstruction of 4–MV bremsstrahlung spectra from measured transmission data. *Med Phys* 10 : 778–785, 1983.
4. Piermattei A, Arcovito G, Azario L, Bacci C, Bianciardi L, Sapio E, Giacco C : A study of quality of bremsstrahlung spectra reconstructed from transmission measurements. *Med Phys* 17 : 227–233, 199.
5. ICRU : Radiation dosimetry : x-ray generated at potentials of 5 to 150 KV. In ICRU Report 17, 1970.
6. Fewell TR, Shuping RE : Handbook of Mammographic X–ray Spectra, HEW(FDA), 1978, pp. 79–80.
7. Baird LC : X–ray spectra vs attenuation data : A theoretical analysis. *Med Phys* 8 : 319–323, 1981.
8. Ahuja SD, Steward PG, Roy TS, Slessinger ED : Estimated spectrum of a 4–MV therapeutic beam. *Med Phys* 13 : 368–373, 1986.
9. Sandifer CW, Taherzadeh M : NaI Spectrometer Measurements of Thick Target Bremsstrahlung at Electron Energies above 5 MeV. In EG & G Tech Rept. 1968, pp. 1–33.
10. Johns HE, Cunningham JR : The Physics of Radiology, 4th ed. Charles C. Thomas, Springfield, 1983, pp. 217–269.
11. Hubbel JH : Photon cross sections, attenuation coefficients, and energy absorption coefficients from 10 keV to 100 GeV. NSRD-NBS 29, Washing D. C. U. S. National Bureau of Standards, 1969.

Laplace transform 방법에 의한 x-ray의 에너지 스펙트럼 추정

유명진

고신의료원 치료방사선과

초 록

Jones 모델 및 HKB모델을 이용하여 Laplace transform방법으로 6MV X-ray의 대략적인 에너지 스펙트럼을 분석하였다.

Jones모델은 투과계수 0.1이하에서는 Laplace transform방법이 적용될 수 없는 심한 제약을 받는다는 것을 알 수 있었다.

HKB모델에 의한 에너지 스펙트럼은 대체로 실제의 에너지 스펙트럼과 일치하는 형태를 나타내지만 6MeV에너지 이상의 영역에서 길게 꼬리를 이루는 단점이 있었다.